CHEMISTRY
A EUROPEAN JOURNAL

DOI: 10.1002/chem.200902993

Self-Discriminating Self-Assembly of Dinuclear Heterochiral Rhombs from Tröger's Base Derived Bis(pyridyl) Ligands

Torsten Weilandt,[a] Ulf Kiehne,[a] Jens Bunzen,[a] Gregor Schnakenburg,[b] and Arne Lützen*[a]

Dedicated to Professor Dr. Uwe Rosenthal on the occasion of his 60th birthday

Abstract: Five racemic dissymmetric bis(pyridyl) ligands based on 2,8- or 3,9-difunctionalised Tröger's base derivatives have been synthesised. Only those derived from a 2,8-difunctionalised scaffold were found to undergo selective self-assembly to discrete self-assembled dinuclear metallosupramolecular aggregates of rhomboid shape upon coordination to *cis*-protected Pd^{2+} or Pt^{2+} ions, as evidenced by ESI mass spectrometry, NMR spectroscopy and single-crystal X-ray diffraction. Interestingly, these processes were found to be highly diastereoselective leading to the formation of C_{2v}-symmetric heterochiral assemblies in a self-discriminating manner.

Keywords: diastereoselectivity · palladium · platinum · self-assembly · supramolecular chemistry

Introduction

The formation of stereochemically defined oligonuclear metallosupramolecular aggregates through stereoselective self-assembly processes has become an increasingly important area of research in recent years.[1] In most approaches, chiral ligands are employed to achieve enantio- or diastereoselective assembly, but these processes are non-trivial in predicting when racemic ligands are used.[1,2] If there is any stereoselection at all there are two different scenarios in cases in which no new stereogenic elements are formed during the self-assembly process, for example, in the case of stereogenic metal centres: either a racemic set of homochiral assemblies is formed in a self-recognition process[3] or an achiral heterochiral assembly is obtained in a self-discrimination process.[4] However, both of these scenarios have been observed in only a few cases so far.[3,4]

Recently, we were able to demonstrate that a racemic bis(nitrile) ligand based on the chiral Tröger's base scaffold undergoes diastereoselective self-assembly to heterochiral aggregates in a self-discriminating manner upon coordination to [(dppp)Pd(OTf)$_2$] or [(dppp)Pt(OTf)$_2$] (dppp = 1,3-bis(diphenylphosphino)propane).[5] This behaviour was rather surprising because racemic bis(2,2′-bipyridyl) derivatives of Tröger's base have been found to undergo stereoselective self-assembly to homochiral dinuclear helicates upon coordination to copper(I) or silver(I) ions.[3g,h,6] Thus, we wanted to study this phenomenon further to see whether this was just an accidental finding or whether it is a more general phenomenon of these kinds of Tröger's base derived ligands. Because bis(pyridyl) ligands are well recognised to form defined metallosupramolecular aggregates upon complexation with square-planar-coordinated palladium(II) or platinum(II) ions as well as other ions,[7] we decided to prepare a series of racemic Tröger's base derived bis(pyridyl) ligands (Scheme 1) with varying substitution patterns and dimensions and to study their self-assembly to metallosupramolecular rhombs upon coordination to [(dppp)Pd(OTf)$_2$] or [(dppp)Pt(OTf)$_2$].

Results and Discussion

Synthesis: Bis(pyridyl) ligand (*rac*)-**1** was prepared from the previously reported 2,8-diamino derivative (*rac*)-**6**[3g] of Trö-

[a] Dr. T. Weilandt, Dr. U. Kiehne, J. Bunzen, Prof. Dr. A. Lützen
University of Bonn
Kekulé-Institute of Oganic Chemistry and Biochemistry
Gerhard-Domagk-Strasse 1, 53121 Bonn (Germany)
Fax: (+49) 228-73-9608
E-mail: arne.luetzen@uni-bonn.de

[b] Dr. G. Schnakenburg
University of Bonn, Institute of Inorganic Chemistry
Gerhard-Domagk-Strasse 1, 53121 Bonn (Germany)

Supporting information for this article is available on the WWW under http://dx.doi.org/10.1002/chem.200902993.

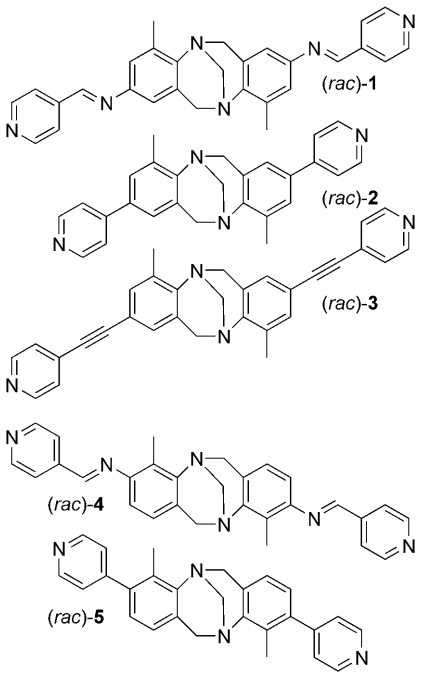

Scheme 1. Tröger's base derived bis(pyridyl) ligands (*rac*)-**1**–**5**.

ger's base by condensation with isonicotinaldehyde (Scheme 2).

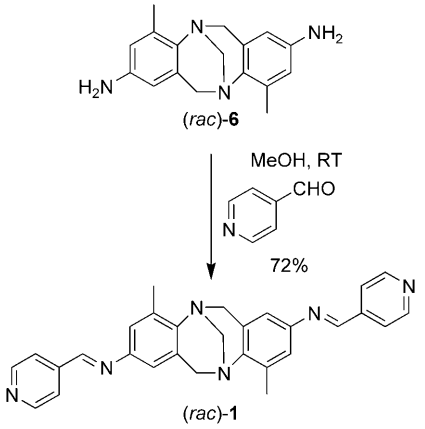

Scheme 2. Synthesis of Tröger's base derived bis(pyridyl) ligand (*rac*)-**1**.

Similarly, ligand (*rac*)-**4** was synthesised by condensation of isonicotinaldehyde with the 3,9-diamino derivative (*rac*)-**8** of Tröger's base, which was prepared starting from 2-methyl-3-nitroaniline by condensation with formaldehyde to synthesise the 3,9-dinitro derivative of Tröger's base (*rac*)-**7** followed by reduction of the nitro functions (Scheme 3).

Ligands (*rac*)-**2**[8] and (*rac*)-**5** were synthesised by Suzuki cross-coupling reactions of 4-pyridylboronic acid with either (*rac*)-2,8-diiodo-4,10-dimethyl-5-11-methano-6*H*,12*H*-dibenzo[*b*,*f*]diazocine ((*rac*)-**9**)[9] or (*rac*)-3,9-dibromo-4,10-dimethyl-5-11-methano-6*H*,12*H*-dibenzo[*b*,*f*]diazocine

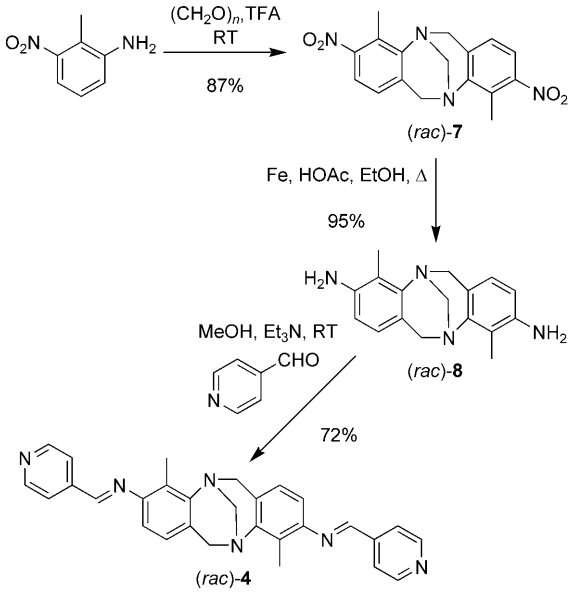

Scheme 3. Synthesis of Tröger's base derived bis(pyridyl) ligand (*rac*)-**4**.

((*rac*)-**10**),[10] respectively (Scheme 4), which can both be prepared in only one step from the corresponding 3- or 4-halogenated *o*-toluidine.

Finally, ligand (*rac*)-**3** with an ethynyl spacer between the pyridine moieties and the Tröger's base scaffold could be prepared by applying Sonogashira conditions starting from

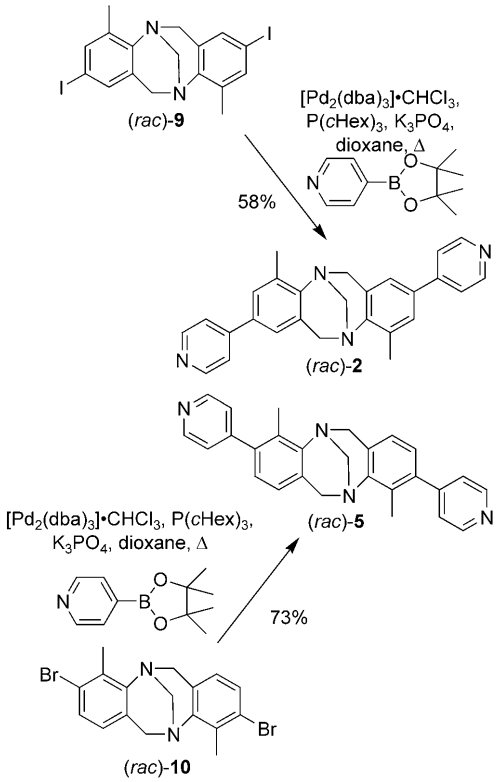

Scheme 4. Synthesis of Tröger's base derived bis(pyridyl) ligands (*rac*)-**2** and (*rac*)-**5**.

(*rac*)-**9** and 4-ethynylpyridine hydrochloride (Scheme 5), similarly to an already published approach.[11]

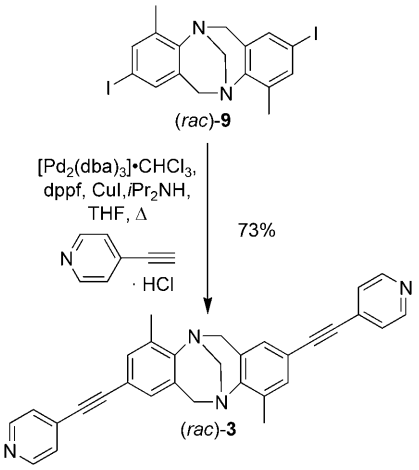

Scheme 5. Synthesis of Tröger's base derived bis(pyridyl) ligand (*rac*)-**3**.

Metal coordination: We then explored the coordination behaviour of these bis(pyridyl) ligands towards Pd^{2+} and Pt^{2+} ions, which typically prefer a square-planar coordination geometry with four donor atoms, that already carry a chelating bis-phosphine ligand and thus offer two *cis*-configured coordination sites to bind two pyridine ligands. $[(dppp)Pd(OTf)_2]$ and $[(dppp)Pt(OTf)_2]$ were used as the precursor complexes and were synthesised according to a published procedure.[12] Mixing stoichiometric amounts of the Tröger's base derived ligands (*rac*)-**1**–**3** carrying the pyridyl groups at the 2,8-positions with the *cis*-configured metal complexes in dichloromethane or acetone resulted in the formation of dinuclear metallosupramolecular rhombs in quantitative yields after 1 hour, as exemplified for ligand (*rac*)-**3** in Scheme 6.

Analysis of the ESI mass spectra of the acetone solutions of the complexes corroborate the formation of dinuclear aggregates, as exemplified for ligand (*rac*)-**3** in Figure 1. The platinum complexes gave spectra showing signals that can be assigned to the expected $\{[(dppp)_2Pt_2(\mathbf{L})_2](OTf)_{4-n}\}^{n+}$ ions, which are generated by the ESI ion source by stripping of one, two, or three counterions (Figure 1a). Not unexpected, in the case of the less stable palladium complexes, a singly charged 1:1 fragment $\{[(dppp)Pd(\mathbf{L})](OTf)\}^+$ (e.g., $m/z = 1120.2$ for $\{[(dppp)Pd(\mathbf{3})](OTf)\}^+$ in Figure 1b) was also detected that has the same m/z ratio as the corresponding intact doubly charged dinuclear rhombs $\{[(dppp)_2Pd_2(\mathbf{L})_2](OTf)_2\}^{2+}$ and thus gives rise to a superpositioned signal. The ionisation conditions are indeed so mild that a signal of a doubly charged ion with a formal composition of $\{[(dppp)_4M_4(\mathbf{L})_4](OTf)_6\}^{2+}$ could also be detected in most cases (e.g., $m/z = 2389.5$ for $\{[(dppp)_4Pd_4(\mathbf{3})_4](OTf)_6\}^{2+}$ in Figure 1b) that is superimposed by the (stronger) signal of a singly charged dinuclear complex that still carries three counterions $\{[(dppp)_2Pd_2(\mathbf{3})_2](OTf)_3\}^+$.

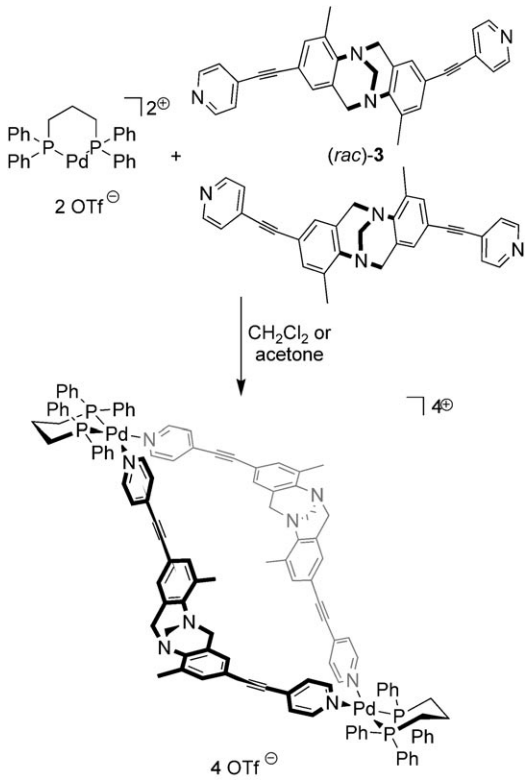

$[(dppp)_2Pd_2\{(5S,11S)\text{-}\mathbf{3}\}\{5R,11R)\text{-}\mathbf{3}\}](OTf)_4$

Scheme 6. Formation of heterochiral metallosupramolecular rhombs by the self-assembly of Tröger's base derived bis(pyridyl) ligand (*rac*)-**3** and $[(dppp)Pd(OTf)_2]$.

However, these result from ESI typical non-specific aggregation of two dinuclear 2:2 complexes rather than from a "real" 4:4 complex because they can easily fragment into two 2:2 complexes but not into any species containing either three ligands or three metal ions. However, the results of the DOSY NMR experiments described below provide further evidence for the exclusive formation of dinuclear metallosupramolecular aggregates.

The ^{1}H NMR spectra of the complexes of ligands **1** and **3** each show only one set of sharp significantly shifted signals (relative to the signals of $[(dppp)M(OTf)_2]$ and the free ligands) at room temperature, which were confirmed as belonging to a single species by 2D NMR techniques. Figures 2 and 3 show the ^{1}H NMR spectra obtained for the palladium and platinum complexes of ligands (*rac*)-**1** and (*rac*)-**3**.

The formation of dinuclear metallosupramolecular aggregates is further strengthened by the interpretation of the ^{31}P NMR spectra of the Pd^{2+} and Pt^{2+} species because the complexes of ligands **1** and **3** show significantly shifted ^{31}P NMR signals, that is, singlets at $\delta = 7.0$ ppm for $[(dppp)_2Pd_2(\mathbf{1})_2](OTf)_4$ and at $\delta = -14.7$ ppm for $[(dppp)_2Pt_2(\mathbf{1})_2](OTf)_4$, whereas the precursor coordination compounds show signals at $\delta = 17.8$ and -11.5 ppm, respectively. Furthermore, the $^1J_{Pt-P}$ coupling constants in the case of the Pt^{II} complexes provide additional proof because it de-

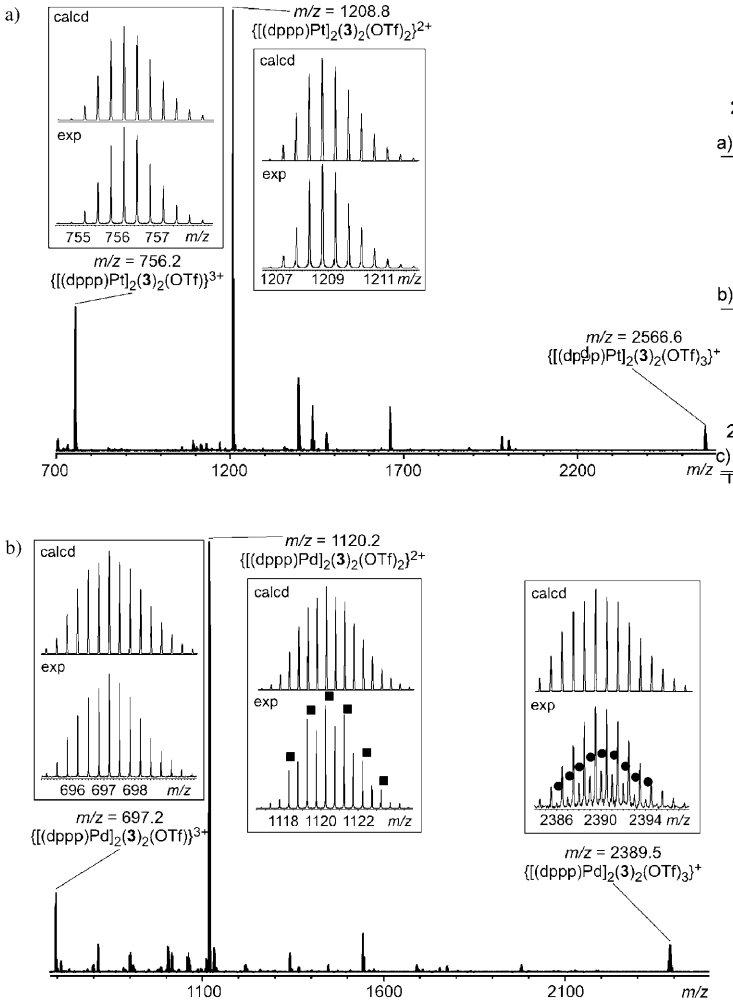

Figure 1. ESI mass spectra (positive mode) of 300 μM acetone solutions of 1:1 mixtures of a) (*rac*)-**3** and [(dppp)Pt(OTf)$_2$] and b) (*rac*)-**3** and [(dppp)Pd(OTf)$_2$]. The insets show the experimental and calculated isotope patterns (calculated on the basis of natural isotope abundances). ■ signals that come from {[(dppp)Pd(**3**)](OTf)}$^+$; ● signals that arise from {[(dppp)$_4$Pd$_4$(**3**)$_4$](OTf)$_6$}$^{2+}$.

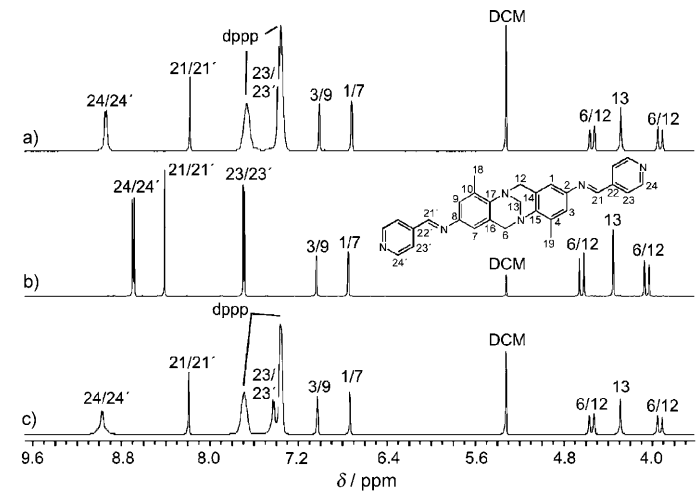

Figure 2. ^{1}H NMR spectra (500.1 MHz, in CD_2Cl_2 at 298 K) of a) (*rac*)-**1** + [(dppp)Pd(OTf)$_2$] (1:1), b) (*rac*)-**1** and c) (*rac*)-**1** + [(dppp)Pt(OTf)$_2$] (1:1).

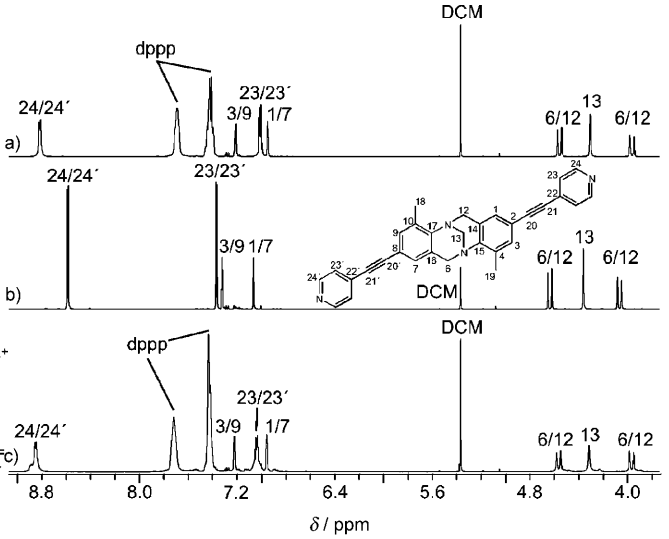

Figure 3. ^{1}H NMR spectra (500.1 MHz, in CD_2Cl_2 at 298 K) of a) (*rac*)-**3** + [(dppp)Pd(OTf)$_2$] (1:1), b) (*rac*)-**3** and c) (*rac*)-**3** + [(dppp)Pt(OTf)$_2$] (1:1).

creases from 3709 Hz for the precursor complex to 3057 Hz for [(dppp)$_2$Pt$_2$(**1**)$_2$](OTf)$_4$.

2D DOSY NMR measurements have also proven to be a valuable tool for investigating self-assembly processes in solution and for gathering information about the actual number and size of different aggregates possibly formed in these processes.[13] As shown representatively for the complexes of **1** in Figure 4, these spectra clearly show that in all cases only one species is present in solution, which is in total agreement with the results obtained from the other NMR spectroscopic and ESI-MS analyses.

Furthermore, we calculated the hydrodynamic radii of these aggregates from the measured diffusion coefficients by employing the Stokes–Einstein equation and correcting the values following the approach of Macchioni et al.[13c] because of the non-spherical, more toroidal shape of our aggregates. These values were found to be in good agreement with those obtained from molecular modelling studies (MM2 force field) and are additional proof that only dinuclear metallosupramolecular rhombs [(dppp)$_2$M$_2$(**L**)$_2$](OTf)$_4$ are formed in solution (Table 1).

Interestingly, the ^{13}C NMR spectra of the dinuclear metallosupramolecular palladium and platinum complexes of ligand (*rac*)-**1** recorded at room temperature are more complicated than we expected compared with the simple ^{1}H and ^{31}P NMR spectra: relative to these we observed almost twice the number of signals in this case. This phenomenon does not occur with ligand (*rac*)-**3** even upon cooling. However, a splitting of the signals of the complexes of (*rac*)-**1** was also observed for the protons at lower temperatures. In principle, there could be three reasons for this: 1) a fast ligand exchange leading to diastereomeric complexes, 2) the presence of *cis*/*trans*-configured isomers of the iminic C=N double bond, or 3) an intramolecular rotation of the C–N single bond. The first possibility is highly unlikely because

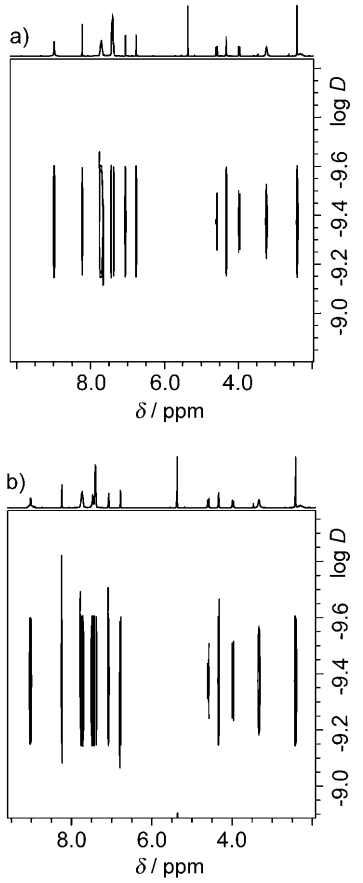

Figure 4. 2D-DOSY NMR spectra (500.1 MHz in CD_2Cl_2 at 298 K) of 1:1 mixtures of a) [(dppp)Pd(OTf)$_2$] and (*rac*)-**1** and b) [(dppp)Pt(OTf)$_2$] and (*rac*)-**1**.

Table 1. Comparison of the experimental and calculated radii of the dinuclear metallosupramolecular rhombs.

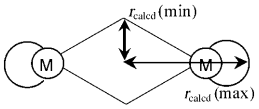

Complex	r_{exp} [nm][a]	r_{calcd} (max.) [nm][b]	r_{calcd} (min.) [nm][b]
[(dppp)$_2$Pd$_2$(**1**)$_2$](OTf)$_4$	1.18	1.49	0.99
[(dppp)$_2$Pt$_2$(**1**)$_2$](OTf)$_4$	1.15	1.49	0.99
[(dppp)$_2$Pd$_2$(**2**)$_2$](OTf)$_4$	1.03	1.33	0.81
[(dppp)$_2$Pt$_2$(**2**)$_2$](OTf)$_4$	1.07	1.33	0.81
[(dppp)$_2$Pd$_2$(**3**)$_2$](OTf)$_4$	1.22	1.50	1.04
[(dppp)$_2$Pt$_2$(**3**)$_2$](OTf)$_4$	1.10	1.50	1.04

[a] Calculated from the measured diffusion constants by applying the Stokes–Einstein equation and correcting these values according to the approach of Macchioni et al.[13c] as a result of their toroidal shape. [b] The radii r_{calcd}(max.) and r_{calcd}(min.) calculated for the long and the short diagonal of the rhomboid assembly's structure obtained by molecular modelling, respectively (MM2 force field, calculated without counterions).

this would demand an intermolecular process involving the breaking and formation of two metal–ligand bonds. In this case one would expect a big difference between the palladium and the platinum complexes due to the difference in bond strength. This, however, is not observed, which suggests that the reason should be an intramolecular process. The second possibility would be possible from this point of view, however, molecular modelling studies suggest that first the energy barrier for this isomerisation process would be far too high and secondly that the *cis* isomer is not sufficiently well preorganised to allow the formation of discrete dinuclear complexes. Further proof for this assumption is the fact that we were not able to detect *cis*/*trans* isomerisation in the free ligand. The rotation around the C–N single bond, however, should be a very fast process in the free ligand. However, within the dinuclear assembly the rotation is definitely slower because it can only occur in a concerted manner within the metallamacrocycle leading to different conformers. This is still fast at room temperature on the ^{1}H and the ^{31}P NMR timescale, but too slow on the ^{13}C NMR timescale.

Similar observations were made for the complexes of ligand (*rac*)-**2**, however, in this case the ^{1}H and the ^{31}P NMR spectra also show signal splitting at room temperature. Again this can be explained by a concerted intramolecular rotation around the aryl–heteroaryl bonds within the ligands, which leads to different rotamers. This process is slow even at room temperature because the groups that have to rotate in a concerted manner are even larger in this case than in the assemblies of ligand (*rac*)-**1**.

Thus, the NMR analyses strongly indicate the highly diastereoselective formation of dinuclear metallosupramolecular rhombs. However, the spectra recorded so far do not allow the two possible stereoisomers, namely the racemic C_2-symmetric homochiral assembly and the achiral C_{2v}-symmetric heterochiral assembly, to be distinguished because the symmetry of the spectra only proves that the assemblies have to be at least C_2-symmetric. Thus, we performed additional experiments with a europium tris[3-heptafluoropropyl(hydroxy)methylene-(+)-camphorate] as a chiral shift reagent and a solution of [(dppp)$_2$Pt$_2$(**3**)$_2$](OTf)$_4$. However, no splitting of the signals could be observed in either the ^{1}H or ^{31}P NMR spectra even upon addition of a larger excess of the chiral shift reagent. Instead we obtained almost unchanged spectra showing only one set of signals for our assembly. This is a good indication that the achiral heterochiral assembly is formed rather than a racemic mixture of homochiral assemblies.

Fortunately we were able to grow crystals of three of the dinuclear metal coordination compounds by slow diffusion of diethyl ether into dichloromethane solutions that were suitable for X-ray single crystal structure analysis. These provide the final proof that our metallosupramolecular aggregates formed from ligands **1**–**3** are indeed heterochiral assemblies [(dppp)$_2$M$_2${(5*S*,11*S*)-**L**}{(5*R*,11*R*)-**L**}](OTf)$_4$ (M = Pd, Pt), as shown in Figures 5 and 6 for the examples of the palladium and platinum complexes of ligands **2** and **3**, respectively.

Clearly it is an inherent property of the 2,8-disubstituted Tröger's base scaffold to induce the diastereoselective formation of heterochiral dinuclear assemblies with [(dppp)M-

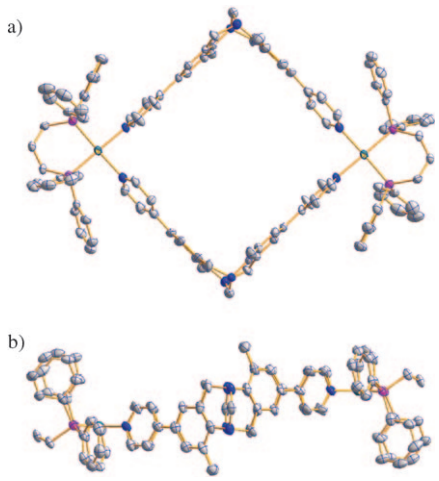

Figure 5. ORTEP plot of the molecular rhomb $[(dppp)_2Pd_2\{(5S,11S)\text{-}\mathbf{2}\}\{(5R,11R)\text{-}\mathbf{2}\}](OTf)_4$ (30% probability of the thermal ellipsoids): a) top view; b) side view. Hydrogen atoms, counterions and solvent molecules have been omitted for clarity. Colour code: grey: carbon; blue: nitrogen; purple: phosphorus; grey-blue: palladium.

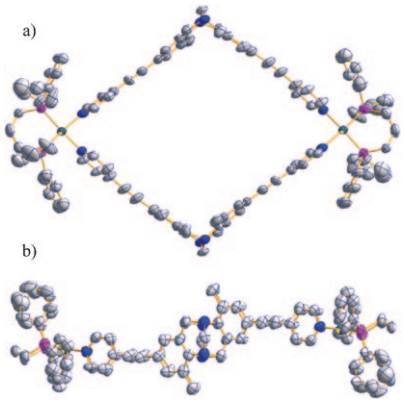

Figure 6. ORTEP plot of the molecular rhomb $[(dppp)_2Pt_2\{(5S,11S)\text{-}\mathbf{3}\}\{(5R,11R)\text{-}\mathbf{3}\}](OTf)_4$ (30% probability of the thermal ellipsoids): a) top view; b) side view. Hydrogen atoms, counterions and solvent molecules have been omitted for clarity. Colour code: grey: carbon; blue: nitrogen; purple: phosphorus; grey-blue: platinum.

$(OTf)_2]$ (M = Pd, Pt) when racemic ligands are used. However, a subtle change in the structure of this kind of ligand, for example, changing the substitution pattern from 2,8 to 3,9, changes the situation completely, as we discovered when we examined the self-assembly of ligands (*rac*)-**4** and (*rac*)-**5** with $[(dppp)M(OTf)_2]$ (M = Pd, Pt). In these cases the ESI mass spectra reveal that the self-assembly processes are not selective (even with regard to the stoichiometry of the assemblies): although signals of the singly, doubly and triply charged cationic $\{[(dppp)_2M_2(\mathbf{L})_2](OTf)_{4-n}\}^{n+}$ (M = Pd, Pt; **L** = **4**, **5**) could be observed a lot of signals were detected that could not be assigned to discrete dinuclear complexes. This is also corroborated by the NMR spectroscopic measurements because the spectra clearly demonstrate that a mixture of aggregates is formed when we examined the coordination behaviour of (*rac*)-**4** or (*rac*)-**5** towards $[(dppp)M(OTf)_2]$ (M = Pd, Pt). This is due to the fact that the 3,9-substitution pattern causes a slightly wider opening angle of the V-shaped structure of the ligand compared with the 2,8-disubstituted isomer, as can be seen from the X-ray crystal structure analyses of ligands (*rac*)-**2** and (*rac*)-**5** (Figure 7). Although the difference is not really big, it is clearly large enough to cause a substantial difference in the degree of preorganisation of the ligands with regard to the stereoselective formation of dinuclear rhombs.

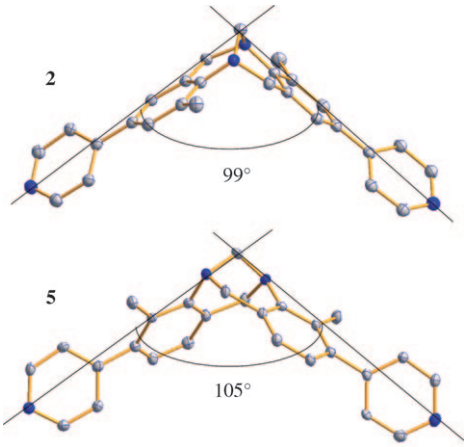

Figure 7. ORTEP plot of ligands (*rac*)-**2** and (*rac*)-**5**. The angles were measured between the two pyridyl nitrogen atoms and the central methylene carbon atom of the Tröger's base scaffold (30% probability of the thermal ellipsoids; only one of the enantiomers is shown in each case. Hydrogen atoms, counterions and solvent molecules have been omitted for clarity. Colour code: grey: carbon; blue: nitrogen.).

Conclusion

We have synthesised five racemic bis(4-pyridyl) ligands (*rac*)-**1**–**5** with both flexible or rigid spacer units and investigated their coordination behaviour towards *cis*-protected Stang-type Pd^{2+} or Pt^{2+} precursor complexes $[(dppp)M(OTf)_2]$ (M = Pd, Pt). In ligands (*rac*)-**4** and (*rac*)-**5** the 3,9-substitution pattern of the Tröger's base core clearly causes an unfavourable preorganisation of the ligand structure, which leads to non-selective self-assembly processes. Changing to a 2,8-substitution pattern in ligands (*rac*)-**1**–**3**, however, leads to well-defined dinuclear assemblies regardless of the increasing size of the ligands and the use of different spacer groups. These aggregates are not only formed selectively with regard to their stoichiometry but also in terms of their stereoselectivity because they exclusively form achiral heterochiral dinuclear metallosupramolecular rhombs in a diastereoselective self-discrimination process that so far has been a rather rare phenomenon.

We are currently investigating the molecular recognition behaviour of these self-assembled aggregates with suitable guest molecules or ions and also trying to prepare the ligands in enantiomerically pure forms to study their self-assembly.

Experimental Section

General: All reactions except the synthesis of (*rac*)-**7** were performed under an argon atmosphere using standard Schlenk techniques and oven-dried glassware. TLC was performed on aluminium TLC plates (silica gel 60 F_{254}) with detection by UV light (254 and 366 nm). The products were purified by column chromatography on silica gel 60 (70–230 mesh). NMR spectra were recorded on a Bruker DRX 500 spectrometer. ^{1}H and ^{13}C NMR spectra were recorded at 298 K at 500.1 and 125.8 MHz, respectively. ^{31}P NMR spectra were recorded at 298 K at 162.0 MHz. ^{1}H NMR chemical shifts are reported on the δ scale (ppm) relative to residual non-deuteriated solvent as the internal standard. ^{13}C NMR chemical shifts are reported on the δ scale (ppm) relative to deuteriated solvent as internal standard. ^{31}P NMR chemical shifts are reported on the δ-scale (ppm) relative to 85% H_3PO_4 as the external standard. Signals were assigned on the basis of ^{1}H, ^{13}C, HMQC and HMBC NMR experiments. EI-mass spectra were taken on an A.E.I. MS-50 (EI; HiRes-EI). ESI-mass spectra were recorded on a Bruker APEX IV FT mass spectrometer. Elemental analyses were carried out with a Heraeus Vario EL. Melting points were measured with a hot-stage microscope SM-Lux from Leitz and are not corrected. Molecular mechanics studies (MM2 force field) were carried out with the CAChe 5.0 program.[14]

Solvents were dried, distilled and stored under argon according to standard procedures whenever necessary. All chemicals were used as received from commercial sources. (*rac*)-2,8-Diamino-4,10-dimethyl-5,11-methano-6*H*,12*H*-dibenzo[*b*,*f*]diazocine ((*rac*)-**6**),[3g] (*rac*)-2,8-diiodo-4,10-dimethyl-5,11-methano-6*H*,12*H*-dibenzo[*b*,*f*]diazocine ((*rac*)-**9**)[9] and (*rac*)-3,9-dibromo-4,10-dimethyl-5,11-methano-6*H*,12*H*-dibenzo[*b*,*f*]diazocine ((*rac*)-**10**)[10] were prepared according to published procedures.

(*rac*)-2,8-Bis(4-pyridylmethyleneamino)-4,10-dimethyl-5,11-methano-6*H*,12*H*-dibenzo[*b*,*f*][1,5]diazocine ((*rac*)-1): Diazocine (*rac*)-**6** (150 mg, 0.54 mmol) was dissolved in methanol (6 mL) ((*rac*)-**6** has to be completely dissolved, if not, more methanol has to be added). 4-Pyridylcarbaldehyde (115 mg, 1.07 mmol, 2 equiv) was added and the resulting yellowish solution was stirred at RT for 22 h. After around 6 h a pale-yellow solid began to precipitate. The precipitate was filtered off, washed with small amounts of cold methanol and dried in vacuo. Yield: 179 mg (0.39 mmol, 72%); m.p. 189–191 °C; ^{1}H NMR (500.1 MHz, CD_2Cl_2): δ = 2.46 (s, 6H; C*H*$_3$), 4.06 (d, ^{2}J = −16.9 Hz, 2H; 6-H*endo*, 12-H*endo*), 4.36 (s, 2H; 13-H), 4.64 (d, ^{2}J = −16.9 Hz, 2H; 6-H*exo*, 12-H*exo*), 6.75 (d, $^{4}J_{1,3}$ = 1.9 Hz, 2H; 1-H, 7-H), 7.04 (d, $^{4}J_{1,3}$ = 1.9 Hz, 2H; 3-H, 9-H), 7.69 (dd, $^{3}J_{\text{H-2Py–H-3Py}}$ = 4.4 Hz, $^{4}J_{\text{H-2Py–H-2'Py}}$ = 1.5 Hz, 4H; 2-H_{Py}, 2'-H_{Py}), 8.41 (s, 2H; N=C*H*), 8.69 (dd, $^{3}J_{\text{H-2Py–H-3Py}}$ = 4.4 Hz, $^{4}J_{\text{H-3Py–H-3'Py}}$ = 1.6 Hz, 4H; 3-H_{Py}, 3′-H_{Py}) ppm; ^{13}C NMR (125.8 MHz, CD_2Cl_2): δ = 17.3 (*C*H$_3$), 55.6 (C-6, C-12), 68.1 (C-13), 117.3 (C-1, C-7), 122.2 (C-3, C-9), 122.4 (C-3$_{Py}$, C-3′$_{Py}$), 129.3 (C-14, C-16), 134.5 (C-4, C-10), 143.3 (C-2$_{Py}$, C-2′$_{Py}$), 145.7 (C-15, C-17), 146.7 (C-2, C-8), 150.9 (C-3$_{Py}$, C-3′$_{Py}$), 157.0 (N=CH) ppm; MS (EI): *m*/*z* (%): 458.2 (100) $[C_{29}H_{26}N_6]^{+\bullet}$; HRMS (EI): calcd for $[C_{29}H_{25}N_6]^{+}$: 457.2135, found: 457.2144; elemental analysis calcd (%) for $C_{29}H_{26}N_6$: C 75.96, H 5.71, N 18.33; found: C 75.66, H 5.98, N 17.98.

(*rac*)-2,8-Bis(4-pyridyl)-4,10-dimethyl-5,11-methano-6*H*,12*H*-dibenzo-[*b*,*f*][1,5]diazocine ((*rac*)-2): 1,4-Dioxane (5 mL) and water (1.4 mL) were added to K_3PO_4 (760 mg, 3.59 mmol, 6 equiv), (*rac*)-2,8-diiodo-4,10-dimethyl-5,11-methano-6*H*,12*H*-dibenzo[*b*,*f*]diazocine ((*rac*)-**9**, 300 mg,0.60 mmol), $[Pd_2(dba)_3]$•$CHCl_3$ (13 mg, 12.0 μmol, 4 mol% Pd), 4-pyridylboronic acid pinacol ester (270 mg, 1.32 mmol, 2.2 equiv) and tris(-cyclohexyl)phosphine (8 mg, 28 μmol, 4.8 mol%). The resulting mixture was degassed and then heated at reflux for 18 h. CH_2Cl_2 was added and the mixture was washed twice with sat. aq. Na_2CO_3. The aqueous layers were extracted twice with CH_2Cl_2 (20 mL) and the combined organic layers were dried over Na_2SO_4. The crude product was purified by column chromatography on silica gel (eluent: toluene/THF (1:1) + 5% Et_3N, R_f = 0.25) to give the desired product as a yellow solid. Yield: 177 mg (0.44 mmol, 73%); m.p. 187–189 °C; ^{1}H NMR (500.1 MHz, CD_2Cl_2): δ = 2.50 (s, 6H; C*H*$_3$), 4.12 (d, ^{2}J = −17.0 Hz, 2H; 6-H*endo*, 12-H*endo*), 4.39 (s, 2H; 13-H), 4.68 (d, ^{2}J = −17.0 Hz, 2H; 6-H*exo*, 12-H*exo*), 7.10 (d, $^{4}J_{1,3}$ = 1.6 Hz, 2H; 1-H, 7-H), 7.38 (d, $^{4}J_{1,3}$ = 1.6 Hz, 2H; 3-H, 9-H), 7.42 (dd, $^{3}J_{\text{H-2Py–H-3Py}}$ = 4.6 Hz, $^{4}J_{\text{H-2Py–H-2'Py}}$ = 1.7 Hz, 4H; 3-H_{Py}, 3′-H_{Py}), 8.55 (dd, $^{3}J_{\text{H-2Py–H-3Py}}$ = 4.6 Hz, $^{4}J_{\text{H-3Py–H-3'Py}}$ = 1.7 Hz, 4H; 2-H_{Py}, 2'-H_{Py}) ppm; ^{13}C NMR (125.8 MHz, CD_2Cl_2): δ = 17.4 (*C*H$_3$), 55.6 (C-6, C-12), 68.0 (C-13), 121.5 (C-3$_{Py}$, C-3′$_{Py}$), 123.3 (C-1, C-7), 127.9 (C-3, C-9), 129.1 (C-14, C-16), 133.6 (C-2, C-8), 134.2 (C-4, C-10), 147.5 (C-15, C-17), 148.1 (C-4$_{Py}$, C-4′$_{Py}$), 150.4 (C-2$_{Py}$, C-2′$_{Py}$) ppm; MS (EI): *m*/*z* (%): 404.2 (100) $[C_{27}H_{24}N_4]^{+\bullet}$; HRMS (EI): calcd for $[C_{27}H_{23}N_4]^{+}$: 403.1917; found: 403.1926; elemental analysis calcd (%) for $C_{27}H_{24}N_4$·2THF·$^{1}/_{2}C_6H_5CH_3$·$^{1}/_{2}H_2O$: C 76.58, H 7.51, N 9.28; found: C 76.76, H 7.54, N 9.18.

(*rac*)-2,8-Bis(4-pyridylethynyl)-4,10-dimethyl-5,11-methano-6*H*,12*H*-dibenzo[*b*,*f*][1,5]diazocine ((*rac*)-3): THF (10 mL) and diisopropylamine (170 mg, 1.67 mmol, 2.4 equiv) were added to (*rac*)-2,8-diiodo-4,10-dimethyl-5,11-methano-6*H*,12*H*-dibenzo[*b*,*f*]diazocine ((*rac*)-**9**; 350 mg, 0.70 mmol), CuI (5 mg, 27.9 μmol, 4 mol%), $[Pd_2(dba)_3]$•$CHCl_3$ (22 mg, 20.9 μmol, 6 mol% Pd), 4-ethynylpyridine hydrochloride (213 mg, 1.53 mmol, 2.2 equiv) and dppf (23 mg, 41.8 μmol). The resulting mixture was stirred at 60 °C for 16 h. Sat. aq. NaCl and CH_2Cl_2 were added. The mixture was filtered over Celite and the residue was washed with CH_2Cl_2. The filtrate was washed with sat. aq. $NaHCO_3$ and the organic layer was dried over Na_2SO_4. The crude product was purified by column chromatography (toluene/THF (4:1) + 5% Et_3N, R_f = 0.40) to give a yellowish solid. Yield: 225 mg (0.50 mmol, 73%); m.p. 204–206 °C; ^{1}H NMR (500.1 MHz, CD_2Cl_2): δ = 2.41 (s, 6H; CH_3), 4.02 (d, ^{2}J = −16.9 Hz, 2H; 6-H*endo*, 12-H*endo*), 4.32 (s, 2H; 13-H), 4.59 (d, ^{2}J = −16.9 Hz, 2H; 6-H*exo*, 12-H*exo*), 7.02 (d, $^{4}J_{1,3}$ = 1.1 Hz, 2H; 1-H, 7-H), 7.28 (d, $^{4}J_{1,3}$ = 1.1 Hz, 2H; 3-H, 9-H), 7.32 (dd, $^{3}J_{\text{H-2Py–H-3Py}}$ = 4.4 Hz, $^{4}J_{\text{H-2Py–H-2'Py}}$ = 1.6 Hz, 4H; 3-H_{Py}, 3′-H_{Py}), 8.54 (dd, $^{3}J_{\text{H-2Py–H-3Py}}$ = 4.4 Hz, $^{4}J_{\text{H-3Py–H-3'Py}}$ = 1.6 Hz, 4H; 2-H_{Py}, 2'-H_{Py}) ppm; ^{13}C NMR (125.8 MHz, CD_2Cl_2): δ = 17.1 (*C*H$_3$), 55.2 (C-6, C-12), 67.7 (C-13), 86.2 (C≡C-C_5H_4N), 94.2 (C≡C-C_5H_4N), 117.1 (C-14, C-16), 125.6 (C-3$_{Py}$, C-3′$_{Py}$), 128.4 (C-1, C-7), 128.8 (C-2, C-8), 131.7 (C-1$_{Py}$, C-1′$_{Py}$), 132.7 (C-3, C-9), 133.9 (C-4, C-10), 147.7 (C-15, C-17), 150.1 (C-3$_{Py}$, C-3′$_{Py}$) ppm; MS (EI): *m*/*z* (%): 452.2 (100) $[C_{31}H_{24}N_4]^{+\bullet}$; HRMS (EI): calcd for $[C_{31}H_{24}N_4]^{+\bullet}$: 452.1995; found: 452.1996; elemental analysis calcd (%) for $C_{31}H_{24}N_4$·$^{1}/_{5}$THF·$^{1}/_{5}C_6H_5CH_3$: C 82.15, H 5.65, N 11.54; found: C 82.28, H 5.64, N 11.55.

(*rac*)-3,9-Bis(4-pyridylmethyleneamino)4,10-dimethyl-5,11-methano-6*H*,12*H*-dibenzo[*b*,*f*][1,5]diazocine ((*rac*)-4): Diazocine (*rac*)-**8** (150 mg, 0.54 mmol) was dissolved in methanol (6 mL) and Et_3N (ca. 8 mL) ((*rac*)-**8** has to be completely dissolved, if not, more Et_3N has to be added). 4-Pyridincarbaldehyde (115 mg, 1.07 mmol, 2 equiv) was added and the resulting yellowish solution was stirred at RT for 22 h. The solution was then concentrated until a yellow precipitate appeared. The flask was stored at −20 °C for 14 h and the precipitate was filtered off, washed with small amounts of cold methanol and dried in vacuo. Yield: 179 mg (0.39 mmol, 72%); m.p. 156–159 °C; ^{1}H NMR (500.1 MHz, CD_2Cl_2): δ = 2.45 (s, 6H; CH_3), 4.04 (d, ^{2}J = −17.0 Hz, 2H; 6-H*endo*, 12-H*endo*), 4.38 (s, 2H; 13-H), 4.64 (d, ^{2}J = −17.0 Hz, 2H; 6-H*exo*, 12-H*exo*), 6.70 (d, $^{3}J_{1,2}$ = 8.2 Hz, 2H; 2-H, 8-H), 6.83 (d, $^{3}J_{1,2}$ = 8.2 Hz, 2H; 1-H, 7-H), 7.76 (dd, $^{3}J_{\text{H-2Py–H-3Py}}$ = 4.4 Hz, $^{4}J_{\text{H-2Py–H-2'Py}}$ = 1.5 Hz, 4H; 3-H_{Py}, 3′-H_{Py}), 8.34 (s, 2H; N=CH), 8.72 (dd, $^{3}J_{\text{H-2Py–H-3Py}}$ = 4.4 Hz, $^{4}J_{\text{H-3Py–H-3'Py}}$ = 1.5 Hz, 4H; 2-H_{Py}, 2'-H_{Py}) ppm; ^{13}C NMR (125.8 MHz, CD_2Cl_2) δ = 12.1 (*C*H$_3$), 55.7 (C-6, C-12), 68.0 (C-13), 113.5 (C-2, C-8), 122.5 (C-3$_{Py}$, C-3′$_{Py}$), 125.1 (C-1, C-7), 126.9 (C-14, C-16), 127.8 (C-4, C-10), 143.4 (C-1$_{Py}$, C-1′$_{Py}$), 147.0 (C-15, C-17), 149.7 (C-3, C-9), 150.9 (C-3$_{Py}$, C-3′$_{Py}$), 157.3 (N=CH) ppm; MS (EI): *m*/*z* (%): 458.2 (100) $[C_{29}H_{26}N_6]^{+\bullet}$; HRMS (EI): calcd for $[C_{29}H_{25}N_6]^{+}$: 457.2135; found: 457.2134; elemental analysis calcd (%) for $C_{29}H_{26}N_6$: C 75.96, H 5.71, N 18.33; found: C 76.20, H 6.03, N 18.12.

(*rac*)-3,9-Bis(4-pyridyl)-4,10-dimethyl-5,11-methano-6*H*,12*H*-dibenzo-[*b*,*f*][1,5]diazocine ((*rac*)-5): 1,4-Dioxane (6 mL) and aq. K_3PO_4 (1.7 mL, 1.27 M, 934 mg, 4.41 mmol, 6 equiv) were added to (*rac*)-3,9-dibromo-4,10-dimethyl-5,11-methano-6*H*,12*H*-dibenzo[*b*,*f*]diazocine ((*rac*)-**10**; 300 mg, 0.73 mmol), $[Pd_2(dba)_3]$•$CHCl_3$ (16 mg, 14.7 μmol, 4 mol% Pd), 4-pyridylboronic acid pinacol ester (332 mg, 1.618 mmol, 2.2 equiv) and tris(cyclohexyl)phosphine (10 mg, 35 μmol, 4.8 mol%). The resulting mixture was heated at reflux for 18 h. CH_2Cl_2 was added and the mixture was washed twice with sat. aq. Na_2CO_3. The aqueous layers were extracted twice with CH_2Cl_2 and the combined organic layers were dried over Na_2SO_4. The crude product was purified by column chromatography on

silica gel (eluent: toluene/THF (1:1) + 5% Et_3N, $R_f = 0.45$). Yield: 293 mg (0.72 mmol, 99%); m.p. >210°C; ^{1}H NMR (500.1 MHz, CD_2Cl_2) $\delta = 2.34$ (s, 6H; CH_3), 4.10 (d, $^2J = -17.0$ Hz, 2H; 6-H*endo*, 12-H*endo*), 4.38 (s, 2H; 13-H), 4.68 (d, $^2J = -17.0$ Hz, 2H; 6-H*exo*, 12-H*exo*), 6.94 (m, 4H; 1-H, 2-H, 7-H, 8-H), 7.25 (m, 4H; 3-H_{Py}, 3′-H_{Py}), 8.61 (m, 4H; 2-H_{Py}, 2′-H_{Py}) ppm; ^{13}C NMR (125.8 MHz, CD_2Cl_2) δ = 14.9 (CH_3), 55.7 (C-6, C-12), 68.1 (C-13), 124.7 (C-3$_{Py}$, C-3′$_{Py}$), 124.8 (C-1, C-7)*, 125.0 (C-2, C-8)*, 128.6 (C-14, C-16), 130.8 (C-4, C-10), 139.4 (C-3, C-9), 147.0 (C-15, C-17), 149.9 (C-2$_{Py}$, C-2′$_{Py}$), 150.1 (C-4$_{Py}$, C-4′$_{Py}$) ppm (* assignments may be interchanged); MS (EI): *m/z* (%): 404.2 (100) $[C_{27}H_{24}N_4]^{+\bullet}$; HRMS (EI): calcd for $[C_{27}H_{23}N_4]^+$: 403.1917; found: 403.1927; elemental analysis calcd (%) for $C_{27}H_{24}N_4 \cdot {}^1/_4THF \cdot {}^1/_4H_2O$: C 78.81, H 6.32, N 13.01;found: C 78.71, H 6.08, N 13.33.

(*rac*)-4,10-Dimethyl-3,9-dinitro-5,11-methano-6*H*,12*H*-dibenzo[*b*,*f*]-[1,5]diazocine ((*rac*)-7): 2-Methyl-3-nitroaniline (5 g, 32.86 mmol) and paraformaldehyde (2.07 g, 69.01 mmol, 2.1 equiv) were dissolved in trifluoroacetic acid (65 mL) to form a black-coloured reaction mixture, which was stirred for 48 h and poured into H_2O (200 mL) to yield an intensely yellow precipitate. Aq. NaOH (6N) was added to this suspension (pH 9). The precipitate was filtered off and suspended in acetone (120 mL) at reflux for 20 min. The mixture was cooled, stored at −20°C for 16 h and the yellow product was removed by filtration. Yield: 4.87 g (14.31 mmol, 87%); m.p. >300°C; ^{1}H NMR (500.1 MHz, [D$_6$]DMSO): $\delta = 2.50$ (s, 6H; CH_3), 4.14 (d, $^2J = -17.8$ Hz, 2H; 6-H*endo*, 12-H*endo*), 4.34 (s, 2H; 13-H), 4.65 (d, $^2J = -17.8$ Hz, 2H; 6-H*exo*, 12-H*exo*), 7.10 (d, $^3J_{1,2} = 8.4$ Hz, 2H; 1-H, 7-H), 7.58 (d, $^3J_{1,2} = 8.4$ Hz, 2H; 2-H, 8-H) ppm; ^{13}C NMR (125.8 MHz, [D$_6$]DMSO): $\delta = 12.9$ (CH_3), 54.7 (C-6, C-12), 66.2 (C-13), 119.0 (C-2, C-8), 125.6 (C-4, C-10), 127.6 (C-14, C-16), 133.8 (C-1, C-7), 147.0 (C-15, C-17), 149.2 (C-3, C-9) ppm; MS (EI): *m/z* (%): 340.1 (100) $[C_{17}H_{16}N_4O_4]^{+\bullet}$; HRMS (EI): calcd for $[C_{17}H_{16}N_4O_4]^{+\bullet}$: 340.1165, found: 340.1172; elemental analysis calcd (%) for $C_{17}H_{16}N_4O_4$: C 59.99, H 4.74, N 16.46; found C 60.02, H 4.88, N 16.36.

(*rac*)-3,9-Diamino-4,10-dimethyl-5,11-methano-6*H*,12*H*-dibenzo[*b*,*f*]-[1,5]diazocine ((*rac*)-8): Diazocine (*rac*)-**7** (2.10 g, 6.20 mmol) and iron powder (4.64 g, 83.1 mmol, 13.5 equiv) were suspended in acetic acid (9.4 mL) and ethanol (100 mL). The reaction mixture was heated at reflux for 12 h and then poured into water. Excess iron was filtered off and the aqueous layer extracted with dichloromethane (5×75 mL). The combined organic layers were washed with sat. aq. $NaHCO_3$ and dried over Na_2SO_4. The crude product was pure according to NMR-spectroscopic analysis. Yield: 1.64 g (5.84 mmol, 95%), m.p. 141–143°C; ^{1}H NMR (500.1 MHz, [D$_6$]DMSO): δ 2.05 (s, 6H; CH_3), 3.67 (d, $^2J = -16.5$ Hz, 2H; 6-H*endo*, 12-H*endo*), 4.13 (s, 2H; 13-H), 4.36 (d, $^2J = -16.5$ Hz, 2H; 6-H*exo*, 12-H*exo*), 4.59 (s, 4H; NH_2), 6.32 (d, $^3J_{1,2} = 8.2$ Hz, 2H; 2-H, 8-H), 6.45 (d, $^3J_{1,2} = 8.2$ Hz, 2H; 1-H, 7-H) ppm; ^{13}C NMR (125.8 MHz, [D$_6$]DMSO): δ 10.8 (CH_3), 54.9 (C-6, C-12), 67.3 (C-13), 110.5 (C-2, C-8), 114.8 (C-4, C-10), 115.8 (C-14, C-16), 123.9 (C-1, C-7), 145.5 (C-15, C-17), 146.1 (C-3, C-9) ppm; MS (EI): *m/z* (%): 280.2 (100) $[C_{17}H_{20}N_4]^{+\bullet}$; HRMS (EI): calcd for $[C_{17}H_{20}N_4]^{+\bullet}$: 280.1682; found: 280.1686; elemental analysis calcd (%) for $C_{17}H_{20}N_4 \cdot 1.5C_2H_5OH$: C 70.78, H 7.78, N 18.01; found: C 70.55, H 7.39, N 17.88.

Preparation and characterisation of the metal complexes: Equimolar amounts of the ligands (*rac*)-**1**, (*rac*)-**2**, (*rac*)-**3**, (*rac*)-**4** or (*rac*)-**5** and [(dppp)Pd(OTf)$_2$] or [(dppp)Pt(OTf)$_2$] were dissolved in CD_2Cl_2 and analysed by NMR spectroscopic methods. Acetone-diluted solutions of the complexes were analysed by ESI-MS methods afterwards. Exemplary analytical data are listed here for the dinuclear assemblies of ligand (*rac*)-**3**. The spectra of all the other assemblies can be found in the Supporting Information.

[(dppp)$_2$Pd$_2${(5*S*,11*S*)-3}{(5*R*,11*R*)-3}](OTf)$_4$: ^{1}H NMR (500.1 MHz, CD_2Cl_2): $\delta = 2.25$ (m, 4H; $PCH_2CH_2CH_2P$), 2.33 (s, 12H; CH_3), 3.17 (m, 8H; $PCH_2CH_2CH_2P$), 3.92 (d, $^2J = -16.6$ Hz, 4H; 6-H*endo*, 12-H*endo*), 4.26 (s, 4H; 13-H), 4.51 (d, $^2J = -16.6$ Hz, 4H; 6-H*exo*, 12-H*exo*), 6.90 (s, 4H; 1-H, 7-H), 6.96 (d, $^3J_{\text{H-2Py–H-3Py}} = 5.8$ Hz, 8H; 2-H_{Py}, 2′-H_{Py}), 7.16 (s, 4H; 3-H, 9-H), 7.37 (m, 24H; $H_{dppp(phenyl)}$), 7.65 (m, 16H; $H_{dppp(phenyl)}$), 8.77 (d, $^3J_{\text{H-2Py–H-3Py}} = 5.8$ Hz, 8H; 3-H_{Py}, 3′-H_{Py}) ppm; ^{13}C NMR (125.8 MHz, CD_2Cl_2): $\delta = 17.0$ (CH_3), 18.0 ($PCH_2CH_2CH_2P$), 21.7 ($PCH_2CH_2CH_2P$), 55.0 (C-6, C-12), 67.6 (C-13), 85.1 ($C{\equiv}C$-C_5H_4N), 99.0 ($C{\equiv}C$-C_5H_4N), 116.3 (C-14, C-16), 121.6 (CF_3), 125.6 (C$_{dppp}$), 127.8 (C-3$_{Py}$, C-3′$_{Py}$), 128.8 (C$_{dppp}$), 129.0 (C-2, C-8), 129.9 (C-1, C-7), 132.6 (C$_{dppp}$), 133.3 (C-3, C-9), 133.5 (C$_{dppp}$), 134.0 (C-4, C-10), 134.9 (C-4$_{Py}$, C-4′$_{Py}$), 148.5 (C-15, C-17), 150.2 (C-2$_{Py}$, C-2′$_{Py}$) ppm; ^{31}P NMR (162.0 MHz, CD_2Cl_2): $\delta = 7.0$ ppm; MS (pos. ESI, acetone): *m/z* (%): 697.2 {[(dppp)$_2$Pd$_2${(5*S*,11*S*)-3}{(5*R*,11*R*)-3}](OTf)}$^{3+}$, 1120.2 {[(dppp)$_2$Pd$_2$-{(5*S*,11*S*)-3}{(5*R*,11*R*)-3}](OTf)$_2$}$^{2+}$, 2389.4 {[(dppp)$_2$Pd$_2$[(5*S*,11*S*)-3}-{(5*R*,11*R*)-3}](OTf)$_3$}$^+$.

[(dppp)$_2$Pt$_2${(5*S*,11*S*)-3}{(5*R*,11*R*)-3}](OTf)$_4$: ^{1}H NMR (500.1 MHz, CD_2Cl_2): $\delta = 2.24$ (m, 4H; $PCH_2CH_2CH_2P$), 2.33 (s, 12H; CH_3), 3.27 (m, 8H; $PCH_2CH_2CH_2P$), 3.92 (d, $^2J = -16.8$ Hz, 4H; 6-H*endo*, 12-H*endo*), 4.27 (s, 4H; 13-H), 4.52 (d, $^2J = -16.8$ Hz, 4H; 6-H*exo*, 12-H*exo*), 6.91 (s, 4H; 1-H, 7-H), 6.99 (d, $^3J_{\text{H-2Py–H-3Py}} = 5.6$ Hz, 8H; 2-H_{Py}, 2′-H_{Py}), 7.18 (s, 4H; 3-H, 9-H), 7.39 (m, 24H; $H_{dppp(phenyl)}$), 7.67 (m, 16H; $H_{dppp(phenyl)}$), 8.80 (d, $^3J_{\text{H-2Py–H-3Py}} = 5.6$ Hz, 8H; 3-H_{Py}, 3′-H_{Py}) ppm; ^{13}C NMR (125.8 MHz, CD_2Cl_2): $\delta = 17.0$ (CH_3), 18.0 ($PCH_2CH_2CH_2P$), 21.6 ($PCH_2CH_2CH_2P$), 55.0 (C-6, C-12), 67.6 (C-13), 85.0 ($C{\equiv}C$-C_5H_4N), 99.8 ($C{\equiv}C$-C_5H_4N), 116.2 (C-14, C-16), 121.6 (CF_3), 124.9 (C$_{dppp}$), 128.3 (C-2$_{Py}$, C-2′$_{Py}$), 128.8 (C-1, C-7), 129.1 (C-2, C-8), 129.8 (C$_{dppp}$), 132.7 (C$_{dppp}$), 133.4 (C-3, C-9), 133.5 (C$_{dppp}$), 134.0 (C-4, C-10), 135.5 (C-4$_{Py}$, C-4′$_{Py}$), 148.7 (C-15, C-17), 150.2 (C-3$_{Py}$, C-3′$_{Py}$) ppm; ^{31}P NMR (162.0 MHz, CD_2Cl_2): $\delta = -14.7$ ($^1J_{\text{Pt–P}} = 3059$ Hz) ppm; MS (pos. ESI, acetone): *m/z* (%): 756.2 {[(dppp)$_2$Pt$_2$[(5*S*,11*S*)-3}{(5*R*,11*R*)-3}](OTf)}$^{3+}$, 1208.8 {[(dppp)$_2$Pt$_2$[(5*S*,11*S*)-3}{(5*R*,11*R*)-3}](OTf)$_2$}$^{2+}$, 2566.6 {[(dppp)$_2$Pt$_2$-{(5*S*,11*S*)-3}{(5*R*,11*R*)-3}](OTf)$_3$}$^+$.

X-ray structure determination: The single-crystal X-ray diffraction studies were carried out on a Nonius Kappa CCD ([(dppp)$_2$Pd$_2$[(5*S*,11*S*)-**2**}-{(5*R*,11*R*)-**2**}](OTf)$_4$, [(dppp)$_2$Pt$_2$[(5*S*,11*S*)-**2**}{(5*R*,11*R*)-**2**}](OTf)$_4$) or a STOE IPDS 2T ((*rac*)-**2**, (*rac*)-**5**, [(dppp)$_2$Pt$_2$[(5*S*,11*S*)-**3**}{(5*R*,11*R*)-**3**}]-(OTf)$_4$) diffractometer at 123(2) K using $Mo_{K\alpha}$ radiation ($\lambda = 0.71073$ Å). Direct methods (SHELXS-97) were used to solve the structures. All non-hydrogen atoms were refined anisotropically using full-matrix least-squares refinement on F^2 (SHELXS-97).[15] The supplementary crystallographic data for this paper can be obtained free of charge from The Cambridge Crystallographic Data Centre via www.ccdc.cam.ac.uk/data_request/cif.

Crystal data for (*rac*)-2: Crystal dimensions 0.50×0.50×0.10 mm, triangular colourless plate, $C_{27}H_{24}N_4$, $M = 404.50$, orthorhombic, space group *Pna*21, $a = 10.0194(6)$, $b = 10.2711(9)$, $c = 20.7129(16)$ Å, $\alpha = 90$, $\beta = 90$, $\gamma = 90°$, $V = 2131.6(3)$ Å^3, $Z = 4$, $\rho = 1.260$ g cm^{-3}, $\mu = 0.076$ mm^{-1}, $F(000) = 856$, 14859 reflections ($2\theta_{max} = 29.16°$) measured (2952 unique, $R_{int} = 0.0735$, completeness = 99.9%), R ($I > 2\sigma(I)$) = 0.0375, wR_2 (all data) = 0.0730. GOF = 0.773 for 283 parameters and 1 restraint, largest diff. peak and hole 0.175/−0.192 e Å^{-3}. CCDC-710926 contains the supplementary crystallographic data for this compound.

Crystal data for (*rac*)-5: Crystal dimensions 0.261×0.092×0.04 mm, colourless rods, $C_{27}H_{24}N_4$, $M = 404.50$, monoclinic, space group $P21/a$, $a = 11.0527(10)$, $b = 13.5732(19)$, $c = 13.6944(16)$ Å, $\alpha = 90$, $\beta = 92.317(8)$, $\gamma = 90°$, $V = 2052.8(4)$ Å^3, $Z = 4$, $\rho = 1.309$ g cm^{-3}, $\mu = 0.080$ mm^{-1}, $F(000) = 856$, 8901 reflections ($2\theta_{max} = 29.17°$) measured (5343 unique, $R_{int} = 0.1460$, completeness = 96.4%), R ($I > 2\sigma(I)$) = 0.0596, wR_2 (all data) = 0.1195. GOF = 0.674 for 282 parameters and 0 restraints, largest diff. peak and hole 0.211/−0.217 e Å^{-3}. CCDC-710927 contains the supplementary crystallographic data for this compound.

Crystal data for [(dppp)$_2$Pd$_2$[(5*S*,11*S*)-2}{(5*R*,11*R*)-2}](OTf)$_4$: Crystal dimensions 0.30×0.20×0.13 mm, colourless blocks, $C_{112}H_{100}F_{12}N_8O_{12}P_4Pd_2S_4$, $M = 2443.01$, triclinic, space group $P\bar{1}$, $a = 11.749(2)$, $b = 15.659(4)$, $c = 19.147(3)$ Å, $\alpha = 89.271(12)$, $\beta = 76.720(11)$, $\gamma = 80.639(9)°$, $V = 3381.6(12)$ Å^3, $Z = 1$, $\rho = 1.169$ g cm^{-3}, $\mu = 0.419$ mm^{-1}, $F(000) = 1218$, 29003 reflections ($2\theta_{max} = 27.39°$) measured (11964 unique, $R_{int} = 0.0862$, completeness = 77.9), R ($I > 2\sigma(I)$) = 0.1097, wR_2 (all data) = 0.3066. GOF = 0.945 for 694 parameters and 21 restraints, largest diff. peak and hole 2.145/−0.741 e Å^{-3}. CCDC-707803 contains the supplementary crystallographic data for this compound.

Crystal data for [(dppp)$_2$Pt$_2$[(5*S*,11*S*)-2}{(5*R*,11*R*)-2}](OTf)$_4$: Crystal dimensions 0.38×0.36×0.19 mm, colourless irregular plate-like crystals, $C_{112}H_{100}F_{12}N_8O_{12}P_4Pt_2S_4$, $M = 2620.30$, triclinic, space group $P\bar{1}$, $a = 12.7155(15)$, $b = 14.013(2)$, $c = 17.835(3)$ Å, $\alpha = 110.509(6)$, $\beta = 99.650(10)$,

$\gamma = 94.797(10)°$, $V = 2899.4(7)$ Å^3, $Z = 1$, $\rho = 1.501$ g cm^{-3}, $\mu = 2.617$ mm^{-1}, $F(000) = 1312$, 20488 reflections ($2\theta_{max} = 26.00°$) measured (10065 unique, $R_{int} = 0.0793$, completeness = 88.3%), R ($I > 2\sigma(I)$) = 0.0853, wR_2 (all data) = 0.2493. GOF = 1.001 for 472 parameters and 295 restraints, largest diff. peak and hole 1.493/−1.795 e Å^{-3}. CCDC-746806 contains the supplementary crystallographic data for this compound.

Crystal data for [(dppp)$_2$Pt$_2${(5*S*,11*S*)-3}{(5*R*,11*R*)-3}](OTf)$_4$: Crystal dimensions 0.50 × 0.075 × 0.02 mm, light-yellowish needles, $C_{120}H_{100}F_{12}N_8O_{12}P_4Pd_2S_4$, $M = 2716.38$, monoclinic, space group $P21/n$, $a = 11.2944(8)$, $b = 45.938(3)$, $c = 12.9801(8)$ Å, $\alpha = 90$, $\beta = 94.411(5)$, $\gamma = 90°$, $V = 6714.7(8)$ Å^3, $Z = 2$, $\rho = 1.344$ g cm^{-3}, $\mu = 2.263$ mm^{-1}, $F(000) = 2720$, 49334 reflections ($2\theta_{max} = 26.85°$) measured (14269 unique, $R_{int} = 0.1086$, completeness = 98.9%), R ($I > 2\sigma(I)$) = 0.0579, wR_2 (all data) = 0.1573. GOF = 0.647 for 588 parameters and 54 restraints, largest diff. peak and hole 0.680/−1.282 e Å^{-3}. CCDC-707804 contains the supplementary crystallographic data for this compound.

Acknowledgements

We are grateful to the Deutsche Forschungsgemeinschaft (SFB 624) for financial support. We thank Michael Peintinger for his assistance with the theoretical calculations.

[1] For some recent reviews, see: a) O. Mamula, A. von Zelewsky, *Coord. Chem. Rev.* **2003**, *242*, 87–95; b) G. Seeber, B. E. F. Tiedemann, K. N. Raymond, *Top. Curr. Chem.* **2006**, *265*, 147–183; c) C. He, Y. Zhao, D. Guo, Z. Lin, C. Duan, *Eur. J. Inorg. Chem.* **2007**, 3451–3463; d) S. J. Lee, W. Lin, *Acc. Chem. Res.* **2008**, *41*, 521–537.

[2] B. J. Holliday, C. A. Mirkin, *Angew. Chem.* **2001**, *113*, 2076–2097; *Angew. Chem. Int. Ed.* **2001**, *40*, 2022–2043.

[3] a) R. Krämer, J.-M. Lehn, A. Marquis-Rigault, *Proc. Natl. Acad. Sci. U.S.A.* **1993**, *90*, 5394–5398; b) D. L. Caulder, K. N. Raymond, *Angew. Chem.* **1997**, *109*, 1508–1510; *Angew. Chem. Int. Ed. Engl.* **1997**, *36*, 1440–1442; c) M. A. Masood, E. J. Enemark, T. D. P. Stack, *Angew. Chem.* **1998**, *110*, 973–977; *Angew. Chem. Int. Ed.* **1998**, *37*, 928–932; d) M. Albrecht, M. Schneider, H. Röttele, *Angew. Chem.* **1999**, *111*, 512–515; *Angew. Chem. Int. Ed.* **1999**, *38*, 557–559; e) T. J. Burchell, R. J. Puddephatt, *Inorg. Chem.* **2006**, *45*, 650–659; f) M. Albrecht, R. Fröhlich, *Bull. Chem. Soc. Jpn.* **2007**, *80*, 797–808; g) U. Kiehne, T. Weilandt, A. Lützen, *Org. Lett.* **2007**, *9*, 1283–1286; h) U. Kiehne, T. Weilandt, A. Lützen, *Eur. J. Org. Chem.* **2008**, 2056–2064.

[4] a) M. Kitamura, S. Okada, S. Suga, R. Noyori, *J. Am. Chem. Soc.* **1989**, *111*, 4028–4036; b) B. Hasenknopf, J.-M. Lehn, G. Baum, D. Fenske, *Proc. Natl. Acad. Sci. U.S.A.* **1996**, *93*, 1397–1400; c) T. W. Kim, M. S. Lah, J.-I. Hong, *Chem. Commun.* **2001**, 743–744; d) R. Wang, M. Hong, D. Yuan, Y. Sun, L. Xu, J. Luo, R. Cao, A. S. C. Chan, *Eur. J. Inorg. Chem.* **2004**, 37–43; e) T. J. Burchell, R. J. Puddephatt, *Inorg. Chem.* **2005**, *44*, 3718–3730.

[5] T. Weilandt, U. Kiehne, G. Schnakenburg, A. Lützen, *Chem. Commun.* **2009**, 2320–2322.

[6] It is important to note, however, that these helicates contain further stereogenic metal centres that are formed during the self-assembly process of the dinuclear coordination compounds.

[7] For some recent reviews, see: a) S. R. Seidel, P. J. Stang, *Acc. Chem. Res.* **2002**, *35*, 972–981; b) F. Würthner, C.-C. You, C. R. Saha-Möller, *Chem. Soc. Rev.* **2004**, *33*, 133–146; c) M. Fujita, M. Tominaga, A. Hori, B. Therrien, *Acc. Chem. Res.* **2005**, *38*, 369–378; d) S. J. Lee, J. T. Hupp, *Coord. Chem. Rev.* **2006**, *250*, 1710–1723; e) V. Maurizot, M. Yoshizawa, M. Fujita, *J. Chem. Soc. Dalton Trans.* **2006**, 2750–2756; f) M. Tominaga, M. Fujita, *Bull. Chem. Soc. Jpn.* **2007**, *80*, 1473–1482; g) D. J. Tranchemontagne, Z. Ni, M. O'Keeffe, O. M. Yaghi, *Angew. Chem.* **2008**, *120*, 5214–5225; *Angew. Chem. Int. Ed.* **2008**, *47*, 5136–5147; h) M. Yoshizawa, J. K. Klosterman, M. Fujita, *Angew. Chem.* **2009**, *121*, 3470–3490; *Angew. Chem. Int. Ed.* **2009**, *48*, 3418–3438.

[8] Ligand (*rac*)-**2** could also be prepared by a Suzuki cross-coupling reaction starting from 4-bromopyridine hydrochloride and a previously reported diboronic acid ester derivative of Tröger's base. However, the yield was considerably lower. For the synthesis of the diboronic acid ester, see: a) U. Kiehne, A. Lützen, *Synthesis* **2004**, 1687–1695; b) U. Kiehne, T. Bruhn, G. Schnakenburg, R. Fröhlich, G. Bringmann, A. Lützen, *Chem. Eur. J.* **2008**, *14*, 4246–4255.

[9] J. Jensen, K. Wärnmark, *Synthesis* **2001**, 1873–1877.

[10] A. Hansson, J. Jensen, O. F. Wendt, K. Wärnmark, *Eur. J. Org. Chem.* **2003**, 3179–3188.

[11] J. Jensen, M. Strozyk, K. Wärnmark, *Synthesis* **2002**, 2761–2765.

[12] a) T. G. Appleton, M. A. Bennett, I. B. Tomkins, *J. Chem. Soc. Dalton Trans.* **1976**, 439–446; b) P. J. Stang, D. H. Cao, S. Saito, A. M. Arif, *J. Am. Chem. Soc.* **1995**, *117*, 6273–6283.

[13] a) Y. Cohen, L. Avram, L. Frish, *Angew. Chem.* **2005**, *117*, 524–560; *Angew. Chem. Int. Ed.* **2005**, *44*, 520–554; b) Y. Cohen, L. Avram, T. Evan-Salem, L. Frish, "Diffusion NMR in Supramolecular Chemistry" in *Analytical Methods in Supramolecular Chemistry* (Ed.: C. A. Schalley), Wiley-VCH, Weinheim, **2007**; c) A. Macchioni, G. Ciancaleoni, C. Zuccaccia, D. Zuccaccia, *Chem. Soc. Rev.* **2008**, *37*, 479–489.

[14] CAChe 5.0, Fujitsu Ltd., Krakow, Poland, **2001**..

[15] G. M. Sheldrick, *Acta Crystallogr. Sect. A* **2008**, *64*, 112–122.

Received: October 29, 2009
Published online: January 14, 2010

